J|A|C|S
COMMUNICATIONS

Published on Web 01/25/2008

Mesoporous Silica Nanospheres as Highly Efficient MRI Contrast Agents

Kathryn M. L. Taylor,† Jason S. Kim,† William J. Rieter,† Hongyu An,‡ Weili Lin,‡ and Wenbin Lin*,†

Departments of Chemistry and Radiology, University of North Carolina, Chapel Hill, North Carolina 27599

Received November 9, 2007; E-mail: wlin@unc.edu

Contrast-enhanced magnetic resonance imaging (MRI) is a noninvasive diagnostic tool that not only provides high resolution anatomical images of soft tissue but also quantitatively assesses disease pathogenesis by measuring up-regulated biomarkers. However, currently used MRI contrast agents are mainly small molecule gadolinium chelates that lack sensitivity and often do not provide satisfactory image contrast enhancement in early disease stages. Nanoparticulate MR contrast agents are much more sensitive owing to the enhanced relaxivity (on per magnetic center basis) as a result of reduced tumbling rates and large payloads of active magnetic centers. For example, Weissleder et al. and others have used iron oxide nanoparticles as T_2 contrast agents to image tumor angiogenesis, inflammation, and gene expression.[1] Lanza, Wickline, and co-workers have developed Gd^{3+}-containing microemulsions as efficient T_1 contrast agents for intravascular MR imaging.[2] Several other Gd^{3+}-containing solid nanoparticles have also been recently evaluated as potential MRI contrast agents.[3,4]

Our recent results indicate that the accessibility of the magnetic center to water molecules is key to designing highly efficient nanoparticulate MR contrast agents,[4] underscoring the need for developing new strategies for the synthesis of nanoparticles that can allow ready access of water molecules to the magnetic centers. Mesoporous materials provide an ideal platform for the development of MR-enhancing hybrid materials due to their high surface areas and tunable pore structures. MCM-41-type materials, for example, possess a hexagonal array of one-dimensional channels with diameters that can be tuned from 2 to 10 nm.[5] More recently, synthetic procedures have been developed for controlling the morphologies of MCM-41 materials,[6] leading to mesoporous silica nanospheres (MSNs) with diameters ranging from 60 to 1100 nm that have been utilized in a variety of applications including catalysis[7] and drug delivery.[8] We surmised that grafting of Gd chelates onto MSNs can provide an ideal platform for designing highly efficient MR contrast agents because of the ability to carry a large payload of Gd centers and the enhanced water accessibility of the Gd chelates. Herein we wish to report the synthesis and characterization of a highly efficient MSN-based MR contrast agent and its applications in in vitro and in vivo MR imaging.

The MSN nanoparticles were synthesized using a surfactant-templated, base-catalyzed condensation procedure.[9] Briefly, cetyltrimethylammonium bromide (CTAB) (0.100 g, 0.274 mmol) was dissolved in 48 mL of distilled water along with 0.35 mL of 2 M NaOH. The solution was heated to 80 °C before adding 0.5 mL of tetraethylorthosilicate (TEOS). The reaction mixture was stirred for an additional 2 h at 80 °C. The particles were isolated by centrifuging and washed with water and ethanol. The surfactant template was then extracted with a 1 wt % solution of NaCl in methanol. SEM and TEM images show that the isolated MSN particles have a mean diameter of 75 nm (Figure 1). The particles exhibit PXRD peaks at 2.8, 4.6, and 5.4° that are characteristic of the (100), (110), and (200) planes of the MCM-41 material, respectively. The surfactant-extracted particles were coated with a Gd−Si−DTTA complex via the siloxane linkage by refluxing the particles and the Gd−Si−DTTA complex in toluene. The resulting MSN−Gd particles were isolated by centrifugation, washed with water, ethanol, and a pH 3 water solution, and finally dialyzed against distilled water to ensure the removal of any free complexes adsorbed in the channels.

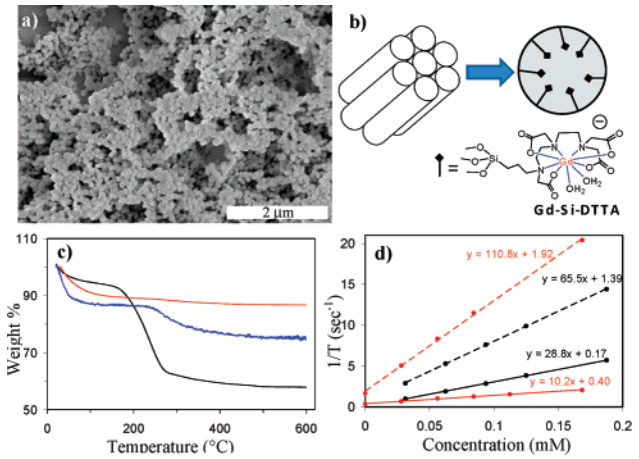

Figure 1. (a) SEM image of MSN showing the formation of monodisperse, water-dispersible nanoparticles. (b) Schematic showing the Gd−Si−DTTA complexes residing in hexagonally ordered nanochannels of ∼2.4 nm in diameter. (c) TGA curves of as-synthesized MSN (black), surfactant-extracted MSN (red), and MSN−Gd (blue). (d) The r_1 (solid) and r_2 (dashed) relaxivity curves of MSN−Gd at 3 T (black) and 9.4 T (red).

SEM and TEM images showed no change of the MSN morphology after the surfactant extraction and upon the grafting of the Gd−DTTA chelate (Supporting Information). TGA results indicated that the CTAB surfactant was completely removed by this procedure as the characteristic weight loss in the 160−290 °C temperature range was absent in the surfactant-extracted MSN (Figure 1c). TGA and direct current plasma spectroscopic results showed that the MSN−Gd material made by this procedure has a consistent Gd−DTTA loading of 15.7−20.1 wt %. Nitrogen gas adsorption measurements indicated that the surfactant-extracted MSN is highly porous with a surface area of 1633 m^2/g and a pore diameter of 2.4 nm, whereas the MSN−Gd material has a reduced surface area of 1470 m^2/g and a pore diameter of 0.9−1.0 nm.

The MR relaxivities of the particles were measured using both a 3.0 T and a 9.4 T MR scanner. The particles exhibited very large longitudinal (r_1) and transverse (r_2) relaxivities. On a per millimolar Gd basis, the particles have an r_1 of 28.8 $mM^{-1}\ s^{-1}$ at 3 T and 10.2 $mM^{-1}\ s^{-1}$ at 9.4 T. The r_2 relaxivities are 65.5 $mM^{-1}\ s^{-1}$ at 3 T and 110.8 $mM^{-1}\ s^{-1}$ at 9.4 T, respectively. The r_1 and r_2 values on a per millimolar particle basis are 7.0×10^5 $mM^{-1}\ s^{-1}$ (3 T)/2.48×10^5 $mM^{-1}\ s^{-1}$ (9.4 T) and 1.6×10^6 $mM^{-1}s^{-1}$ (3 T)/2.7×10^6 (9.4 T), respectively. These relaxivity values are much larger

† Department of Chemistry.
‡ Department of Radiology.

10.1021/ja710193c CCC: $40.75

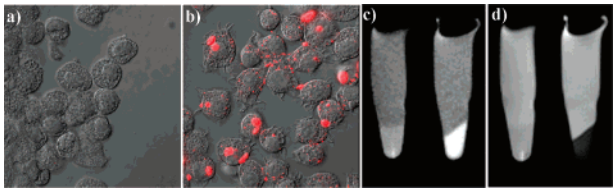

Figure 2. Overlaid DIC and fluorescence image of monocyte cells incubated with (a) no MSN−Gd-1 and (b) 4 μg of MSN−Gd-1 (5×10^{-5} cells in 2 mL medium) (60× magnification). (c) T_1-weighted MR images of monocyte cell pellets incubated without MSN−Gd (left) and with 0.3 mg of MSN−Gd for 5×10^6 cells in 3 mL of media (right). (d) T_2-weighted MR images of monocyte cell pellets incubated without MSN−Gd (left) and with 0.3 mg of MSN−Gd for 5×10^6 cells in 3 mL of media (right).

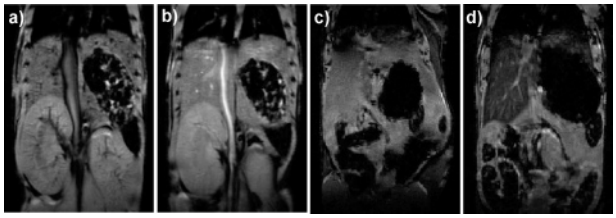

Figure 3. (a) Precontrast and (b) postcontrast (2.1 μmol/kg dose) T_1-weighted mouse MR image showing aorta signal enhancement. (c) Precontrast and (d) post-contrast (31 μmol/kg dose) mouse MR images showing liver signal loss due to T_2-weighted enhancement.

than the solid silica nanoparticles that are coated with multilayers of the Gd−DTPA derivative that was recently reported by our group.[3a] We attributed the enhanced MR relaxivity to the ready access of water molecules through the nanochannels of the MSN−Gd particles.

We have also prepared fluorescently labeled nanoparticles (MSN−Gd-1) by adding 4 mol % of rhodamine B-aminopropyltriethoxysilane (relative to Gd−Si−DTTA) during the coating reaction (Supporting Information). An immortalized murine monocyte cell line was used for the in vitro study because of its phagocytic capacity.[10] Laser scanning confocal fluorescence microscopic studies indicated the efficient uptake of MSN−Gd-1 by monocyte cells (5×10^{-5}) after they were incubated with 2 mL of medium containing 4 μg of MSN−Gd-1 for 0.5 h. The rhodamine B fluorescence is clearly visible in the confocal image of monocyte cells incubated with MSN−Gd-1 but completely absent in the confocal image of monocyte cells alone. We have observed significant MR image enhancement of the labeled monocytes when compared with a control of unlabeled monocytes. To prepare the cells for MR imaging, we incubated $\sim 5 \times 10^6$ cells in 3 mL of media containing 0.3 mg of MSN−Gd for 1 h. The cells were isolated, washed twice with fresh media, pelleted, and finally covered with 200 μL of saline solution. As shown in Figure 2c and 2d, significant positive signal enhancement in the T_1-weighted image and negative signal enhancement in the T_2-weighted image were observed for the labeled cells, depending on the MR pulse sequence employed. The T_1- and T_2-weighted image enhancements were corroborated with the reduction of T_1 and T_2 relaxation times observed on the relaxation time maps (Supporting Information). MTS cell viability assays showed that MSN−Gd nanoparticles were not toxic to monocyte cells; they were completely viable even after incubation with a nanoparticle loading of 10 μg per 5000 monocyte cells for 26 h. More than 85% cells were viable after incubating with 100 μg of MSN−Gd per 5000 cells for 26 h.

We have also evaluated the effectiveness of MSN−Gd as an in vivo MR contrast agent using a 9.4 T scanner. Upon tail vein injection of 2.1 μmol/kg of body weight of MSN−Gd, a significant T_1-weighted enhancement is clearly visible in the aorta of a DBA/1J mouse 15 min post injection (Figure 3b), indicating the utility of MSN−Gd as an intravascular MR contrast agent. This dose level is much lower than what is typically required of currently used contrast agents (0.1−0.3 mmol/kg).[11] We have also shown that MSN−Gd can be an efficient T_2-weighted contrast agent at a higher dosage. After tail injection of 31 μmol/kg, significant loss of MR signal was observed in the liver of the DBA/1J mouse 1 h post injection, indicating the ability of MSN−Gd to enhance T_2-weighted images. The liver signal loss is probably a result of phagocytosis of the MSN−Gd by the liver macrophage cells, as already shown by the efficient uptake of the MSN−Gd by the related monocyte cells. This result suggests the possibility of using MSN−Gd for MR imaging of liver abnormalities such as liver tumors which can be currently carried out with iron oxide nanoparticles.[12]

In summary, we have designed and characterized hybrid mesoporous silica nanospheres (MSN−Gd) with extraordinary ability to enhance MR images. Their utility as contrast agents for optical and MR imaging has been clearly demonstrated in vitro. We have also shown that MSN−Gd is a highly efficient T_1 contrast agent for intravascular MR imaging and an excellent T_2 contrast agent for MR imaging of soft tissues when applied at a higher dosage. We are currently evaluating the potential of utilizing this class of hybrid nanomaterials as target-specific contrast agents for multimodal imaging of cancers and inflammatory arthritis in mice.

Acknowledgment. We acknowledge financial support from NIH (U54-CA119343 and P20 RR020764). We thank Ms. Leah Pranger and Ms. Christie Okoruwa for experimental help. J.S.K. acknowledges the UNC Graduate School for a Dissertation Completion Fellowship, and W.J.R. thanks NSF for a graduate fellowship. W.L. is a Camille Dreyfus Teacher-Scholar.

Supporting Information Available: Experimental procedures and 15 figures. This material is available free of charge via the Internet at http://pubs.acs.org.

References

(1) Weissleder, R.; Moore, A.; Mahmood, U.; Bhorade, R.; Benveniste, H.; Chiocca, E. A.; Basilion, J. P. *Nat. Med.* **2000**, *6*, 351.
(2) Morawski, A. M.; Lanza, G. A.; Wickline, S. A. *Curr Opin. Biotechnol.* **2005**, *16*, 89.
(3) (a) Frias, J. C.; Ma, Y.; Williams, K. J.; Fayad, Z. A.; Fisher, E. A. *Nano Lett.* **2006**, *6*, 2220−2224. (b) Yang, H.; Santra, S.; Walter, G. A.; Holloway, P. H. *Adv. Mater.* **2006**, *18*, 2890−2894.
(4) (a) Rieter, W. J.; Kim, J. S.; Taylor, K. M. L.; An, H.; Lin, W.; Tarrant, T.; Lin, W. *Angew. Chem.* **2007**, *46*, 3680−3682. (b) Kim, J. S.; Rieter, W. J.; Taylor, K. M. L.; An, H.; Lin, W.; Lin, W. *J. Am. Chem. Soc.* **2007**, *129*, 8962−8963.
(5) (a) Kresge, C. T.; Leonowicz, M. E.; Roth, W. J.; Vartuli, J. C.; Beck, J. S. *Nature* **1992**, *359*, 710−712. (b) Beck, J. S.; Vartuli, J. C.; Roth, W. J.; Leonowicz, M. E.; Krege, C. T.; Schmitt, K. D.; Chu, C. T.-W.; Olson, D. H.; Sheppard, E. W.; McCullen, S. B.; Higgins, J. B.; Schlenker, J. L. *J. Am. Chem. Soc.* **1992**, *114*, 10834−10843.
(6) (a) Grün, M.; Unger, K. K.; Matsumoto, A.; Tsutsumi, K. *Microporous Mesoporous Mater.* **1999**, *27*, 207−216. (b) Cai, Q.; Luo, Z.-S.; Pang, W.-Q.; Fan, Y.-W.; Chen, X.-H.; Cui, F.-Z. *Chem. Mater.* **2001**, *13*, 258−263.
(7) Chen, H.-T.; Huh, S.; Wiench, J. W.; Pruski, M.; Lin, V. S.-Y. *J. Am. Chem. Soc.* **2005**, *127*, 13305−13311.
(8) (a) Slowing, I.; Trewyn, B. G.; Lin, V. S.-Y. *J. Am. Chem. Soc.* **2006**, *128*, 14792−14793. (b) Slowing, I.; Trewyn, B. G.; Lin, V. S.-Y. *J. Am. Chem. Soc.* **2007**, *129*, 8845−8849.
(9) Lai, C.-Y.; Trewyn, B. G.; Jeftinija, D. M.; Jeftinija, K.; Xu, S.; Jeftinija, S.; Lin, V. S.-Y. *J. Am. Chem. Soc.* **2003**, *125*, 4451−4459.
(10) Ma, Y.; Pope, R. M. *Curr. Pharm. Des.* **2005**, *11*, 569.
(11) T_1-weighted enhancement of rabbit aorta was elegantly demonstrated with graphite-coated FeCo nanoparticles at a 9.6 μmol/kg dose. Seo, W. S.; Lee, J. H.; Sun, X.; Suzuki, Y.; Mann, D.; Liu, Z.; Terashima, M.; Yang, P. C.; McConnell, M. V.; Nishimura, D. G.; Dai, H. *Nat. Mater.* **2006**, *5*, 971−976.
(12) Reimer, P.; Tombach, B. B. *Eur. Radiol.* **2003**, *13*, 1266−1276.

JA710193C